JOURNAL OF APPLIED ELECTROCHEMISTRY 21 (1991) 1013–1022

Corrosion behaviour of lead-copper alloys in sulphuric acid for battery applications

S. SHAH, R. N. GRUGEL, B. D. LICHTER

Department of Materials Science and Engineering, Vanderbilt University, Nashville, TN 37235, USA

Received 6 July 1990; revised 11 January 1991

The corrosion behaviour in sulphuric acid of monotectic Pb–63 wt % Cu, hyper-monotectic Pb–30 wt % Cu, and Pb–10 wt % Cu was investigated and compared to that of Cu, Pb, as well as Pb–Ca, and Pb–Ca–Sn battery-grid alloys. On anodic polarization of pure Cu and Pb–Cu alloys, dissolution of the copper phase markedly increases as the potential is increased above the Cu/Cu^{2+} reversible potential, which is above the passive potential for lead and lead battery-grid alloys. A limiting current and pseudo-passive transition attains, and the pseudo-passive current decreases with decreasing bulk copper content of the alloy. Extensive selective leaching of copper from the 30 wt % Cu alloy produced a highly porous layer of spongy lead, and the subsequent anodic polarization behaviour (without repolishing the sample surface) showed a reduction in pseudo-passive corrosion rates to values ~ 20 times greater (referred to unit geometric area) than the passive current of pure Pb and lead battery-grid alloys. This difference was attributed partly to dissolution of redeposited copper but mainly to the large effective surface area of the remaining porous lead network. The possible use of Pb–Cu alloys as high-conductivity battery-grid alloys is discussed.

1. Introduction

During the 1970s, Pb–Sb alloys usually containing 4 to 12 wt % Sb were used as grid materials in lead–acid batteries. In recent years, these are being replaced by Pb–Ca alloys which are found to be more suitable because of the elimination of the "gassing" problem. In these alloys, grain-size and the distribution of the precipitates are important factors for sound grids which are able to resist corrosion and grid growth. The addition of Sn improves the mechanical properties and consequently, the cycle-life of a battery. At present such Pb–Ca–Sn alloys have found use mainly as positive grids in "maintenance-free" SLI batteries.

The search for alloys which may improve the efficiency of the battery still continues. Introducing a more conductive grid would reduce the size and the weight of the battery. With the existing system, an easy way of improving the conductivity and hence the efficiency is to incorporate a continuous high conductivity metal phase into essentially pure lead. On possible candidate is the Pb–Cu alloy system. This paper investigates the electrochemical behaviour of this alloy system over a broad composition range with the objective in mind of its possible future use as a commercial battery grid.

The Pb–Cu system displays a liquid–liquid miscibility gap [1] and the associated monotectic reaction (Liquid 1 = Solid 1 + Liquid 2). Employing directional solidification techniques, the behaviour and subsequent microstructure of monotectic and near-monotectic alloys has been characterized by several investigators [2–4]. Unfortunately, density differences and preferential wetting characteristics of the individual liquids often leads to macrosegregation during solidification processing, especially in hypermonotectic alloys.

A detailed study of the solidification aspects of alloys containing 10, 20, 30, 40, and 50 wt % Cu has been completed and presented elsewhere [5]. The goal was first to obtain a structure which incorporates high conductivity copper as a contiguous network in the matrix and then study the corrosion behaviour of such a microstructure. Two representative microstructures (the details of which are given later) obtained from the previous study were selected for electrochemical investigations. Their corrosion properties, along with those of an as-cast monotectic Pb–63 wt % Cu alloy, are compared with those of pure Pb, Pb–Ca and Pb–Ca–Sn alloys, and pure Cu.

2. Experimental details

2.1. *Materials and sample preparation*

Table 1 lists the compositions and treatments of materials investigated. Table 2 lists the concentrations and specific gravities of sulphuric acid used in the investigation. The Pb–Ca, and Pb–Ca–Sn alloys were received in their cast and rolled condition from General Motors, Delco Remy Division. Pure lead (99.999 wt %) was obtained from American Smelting and Refining Company in the form of an ingot which was subsequently rolled and annealed at room temperature. Pure copper (99.999%) in sheet form was also supplied by General Motors, Delco Remy Division. The monotectic Pb–Cu alloy was provided by Dr T. S.

0021-891X/91 $03.00 + .12 © 1991 Chapman & Hall

Table 1. Compositions of materials used

Sample	*Pb* (*% wt*)	*Ca* (*% wt*)	*Sn* (*% wt*)	*Cu* (*% wt*)	*Al* (*p.p.m.*)	*Others*	*Treatment*
Pb	99.99	–	–	–	–	Rest	Cast
Pb–Ca	Rest	0.06	–	–	–	–	Cast and Rolled
Pb–Ca–Sn	Rest	0.08	0.56	–	66	–	Cast and Rolled
Pb–63% Cu	34	–	3	63	–	–	Cast
Cu	–	–	–	99.99	–	Rest	Cast and Rolled
Pb–30% Cu	70	–	–	30	–	–	Directionally solidified
Pb–10% Cu	90	–	–	10	–	–	Directionally solidified

Sudarshan of Synertec Company. Hypermonotectic alloys containing 30 and 10 wt % Cu were cast and subsequently directionally solidified [5].

Further description of these two hypermonotectic alloys is instructive. One sample which originally had 30 wt % Cu was directionally solidified in normal gravity at a pull rate of 1 mm min^{-1} in a gradient of 160 K cm^{-1}. This sample showed segregation, one zone consisting of the copper-rich monotectic microstructure and the other zone containing *aligned* copper dendrites in a lead matrix. The composition of the latter was estimated to be between 15 and 20 wt % Cu. This latter microstructure, shown in Fig. 1a, was selected for further investigation of the corrosion behaviour and is identified by the nominal composition, Pb–30 wt % Cu. The Pb–10 wt % Cu alloy was directionally solidified at a pull rate of 1 mm min^{-1} in a gradient of 160 K cm^{-1} in a cyclicly varying gravity environment which resulted in *dispersed* copper dendrites as seen in Fig. 1b. Solidification was carried out aboard an aircraft which underwent parabolic excursions giving ≈ 20 s of low gravity ($g = 0.01$) followed by ~ 90 s of high gravity ($g = 1.8$). Fig. 1c shows the microstructure of as-cast (i.e., not directionally solidified) Pb–63 wt % Cu alloy for comparison with those of the hypermonotectic alloys.

Samples for corrosion tests and for metallographic examination were cut and mounted in an epoxy resin. Only longitudinal sections were prepared for corrosion tests, for which case a wire was soldered to the sample prior to sealing in the epoxy. For metallography both longitudinal and transverse (perpendicular to the growth direction and to the corroded surface) sections were prepared. The mounted specimens were conventionally ground and polished. The final polishing employed either a cerium oxide suspension in a lubricating soap solution or a 0.05 μm alumina suspension. After polishing the samples were rinsed in deionized water and dried in air.

2.2. *Electrochemical corrosion tests*

The cell used in the experiments was a sealed system consisting of the sample as working-electrode, two platinum counter-electrodes, an external reference electrode coupled to the cell through a salt-bridge/luggin probe, and a gas inlet and outlet. The cell was connected to a model 173 PARC potentiostat and PARC 276 interface to an Apple IIe computer. The PARC Model 332 "Softcorr" program was used to conduct potentiodynamic experiments. The electrolytes were prepared by diluting an initial 1.84 specific gravity sulphuric acid with doubly-distilled deionized water. The cell was purged with nitrogen prior to and

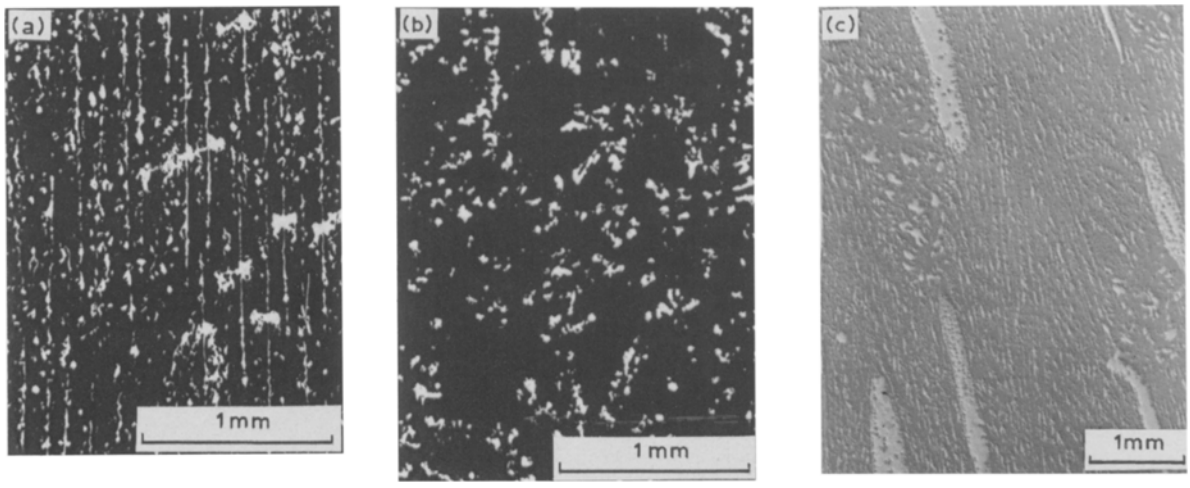

Fig. 1. (a) Microstructure of the lead-rich zone of an Pb–30 wt % Cu alloy directionally solidified in unit gravity at a pull-rate of 1 mm min^{-1} in a gradient of 160 K cm^{-1} showing *aligned* copper dendrites (light phase.) (b) Microstructure of Pb–10 wt % Cu alloy directionally solidified at a pull rate of 1 mm min^{-1} in a gradient of 160 K cm^{-1} in the KC-135 cyclic gravity environment showing *dispersed* copper dendrites. (c) Microstructure of monotectic Pb–63 wt % Cu alloy compared with those of (a) and (b); note that lead particles are incorporated in an aligned copper matrix (dark phase.)

Table 2. Concentration of sulphuric acid

Solution	*Molality*	*Relative density*	*Log M*
1	0.5	1.032	−0.301
2	1.085	1.065	0.0354
3	4.72	1.27	0.674

during the experiment. The potentials were measured against a saturated Hg/Hg_2SO_4 (mercury/mercurous sulphate) reference electrode (+650 mV/NHE) and were anodically scanned from the rest potential at 0.2 mV s^{-1}. All the tests were conducted at room temperature (25° C). Three kinds of tests were carried out:

(i) Anodic polarization tests were performed in 0.5 M (1.0 N), 1.085 M (2.17 N), and 4.72 M (9.44 N) H_2SO_4, except for the hypermonotectic Pb–Cu alloys, which were studied only in the 4.72 M acid. For Pb and lead battery-grid alloys the anodic scan was begun after holding the sample on open circuit until a stable value of E_{corr} was attained. In some instances the scan was started a few millivolts below this potential. For Pb–Cu alloys, the anodic scan was begun immediately on immersion. (See Discussion section below.)

(ii) For the 30 and 10 wt % Cu alloys, the samples were repolished after anodic polarization and then "conditioned" by holding at 0 mV for 60 000 s, during which time the copper phase was selectively leached from the surface while the lead remained in the passive state. The transient current was recorded during leaching and was found to be oscillatory for both samples. The final quasi steady-state current density for Pb–30 wt % Cu was ~0.4 mA cm^{-2} and about ~0.2 mA cm^{-2} for Pb–10 wt % Cu.

(iii) After leaching, the "conditioned" Pb–30 wt % Cu alloy was further investigated for its anodic polarization behaviour by reimmersing in fresh solution and anodically scanning from E_{corr}.

Table 3. Quantitative results for anodic polarization of pure Cu in various acid concentrations

Parameter	*Units*	*0.5 M*	*1.085 M*	*4.72 M*
Anodic Tafel slope	mV $decade^{-1}$	33.4	37.0	39.0
I_c	mA cm^{-2}	134	164	101
E_{corr}	mV	−424	−518	−572
E_{pp}	mV	264	−70	−276
I_p min	mA cm^{-2}	100	90	17.4

3. Results

3.1. *Pure lead and lead battery-grid alloys*

Results are shown in Figs 2–4 and Table 5. The corrosion potential is the $Pb/PbSO_4$ reversible potential, which is highly non-polarizable. A characteristic and highly reproducible active/passive transition occurs due to thickening of the sulphate layer. Additional details have been presented elsewhere [6].

3.2. *Pure copper and Pb–Cu alloys*

Figures 2–4 compare the anodic polarization behaviour of copper and monotectic copper–lead alloy with pure lead and lead battery-grid alloys in 0.5 M, 1.085 M, and 4.72 M sulphuric acid. Figure 5 compares the behaviour of pure copper at all three acid concentrations. Figure 6 is a similar comparison for the Pb–63 wt % Cu alloy. Results for these Pb–30 wt % Cu and Pb–10 wt % Cu alloys together with those for pure Cu in 4.72 M acid are shown in Fig. 7.

The quantitative results for pure copper, the monotectic alloy, and hypermonotectic Pb–Cu alloys are summarized in Tables 3, 4, and 6, respectively. Comparable data for pure lead and lead battery-grid alloys are shown in Table 5. Figure 8 defines and explains the parameters (I_c, I_p, E_{corr}, E_{pp}) used in the following

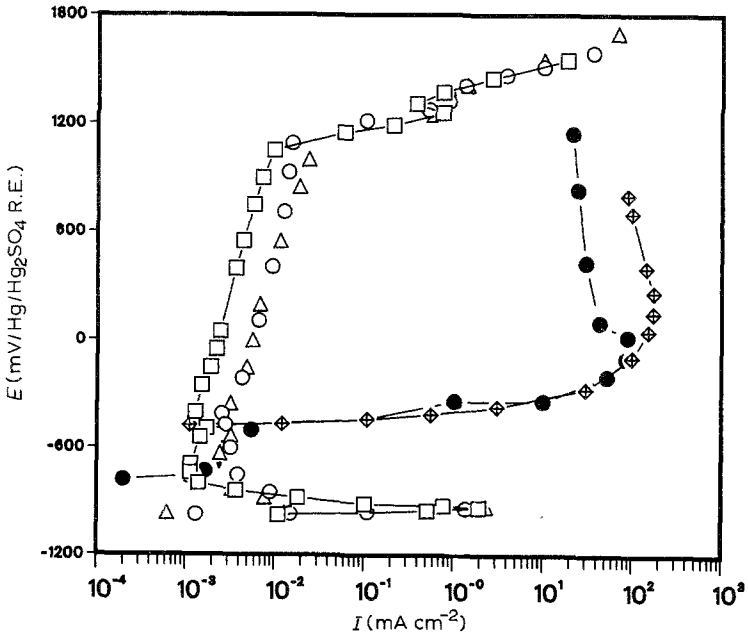

Fig. 2. Anodic polarization of (□) pure Pb, (○) Pb–Ca, (△) Pb–Ca–Sn alloy, (◇) pure Cu, and (■) Pb–63 wt % Cu alloy in 0.5 M (1.0 N) H_2SO_4.

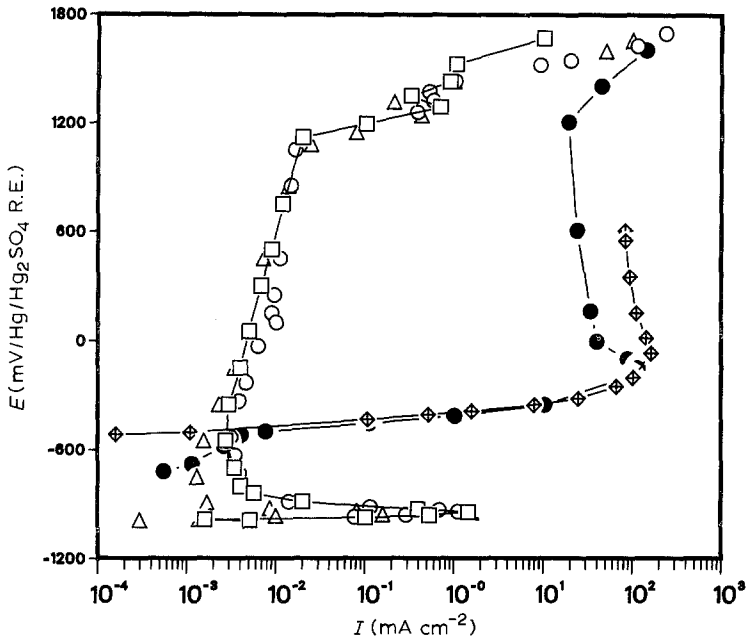

Fig. 3. Anodic polarization of (□) pure Pb, (○) Pb–Ca, (△) Pb–Ca–Sn alloy, (⊕) pure Cu, and (■) Pb–63 wt % Cu alloy in 1.085 M (2.17 N) H_2SO_4.

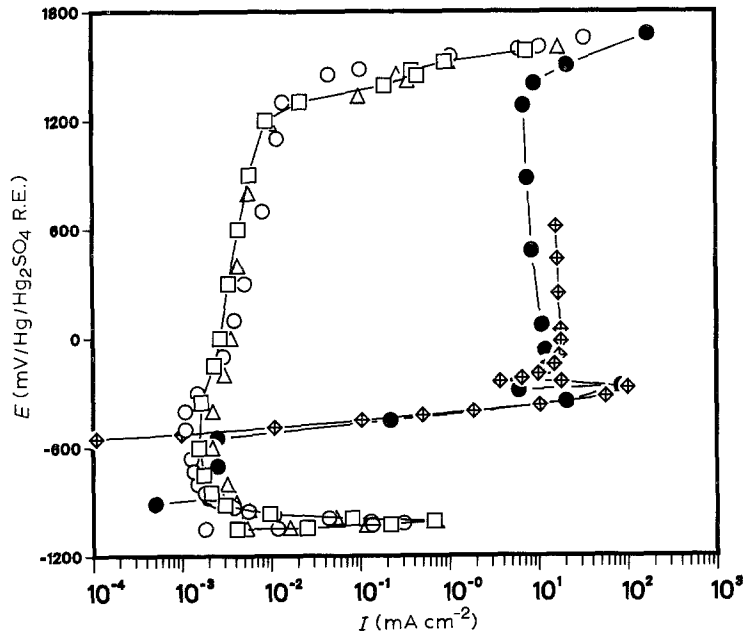

Fig. 4. Anodic polarization of (□) pure Pb, (○) Pb–Ca, (△) Pb–Ca–Sn alloy, (⊕) pure Cu, and (■) Pb–63 wt % Cu alloy in 4.72 M (9.44 N) H_2SO_4.

quantitative comparison of the results:

1. E_{corr} for copper corresponds to a reversible Cu/Cu^{2+} potential (see discussion below) and decreases with increasing acidity. For Pb–Cu alloys, E_{corr} lies between that for pure copper and pure lead and decreases with increasing acid concentration, as does that for pure lead [6]. However, recent findings [7] indicate that these potentials are not steady-state values, and that the alloys revert to an active state with potentials near the values for pure lead, as shown in Figure 9. At higher anodic potentials the alloys resemble pure copper in their behaviour.

2. The I_c values for pure copper and the Pb–Cu alloys are two orders of magnitude greater than those for

Table 4. Quantitative results for anodic polarization of Pb–63 wt % Cu alloy in various acid concentrations

Parameter	*Units*	*0.5 M*	*1.085 M*	*4.72 M*
Tafel slope in the region of copper dissolution	mV decade^{-1}	43	41	46
I_c	mA cm^{-2}	105	117	85.5
E^*_{corr}	mV	−782	−850	−910
E_{pp}	mV	−20	−140	−266
I_p min	mA cm^{-2}	32	23	9.2

* Non steady-state values. With sufficient time, E_{corr} for Pb is attained. See Fig. 9.

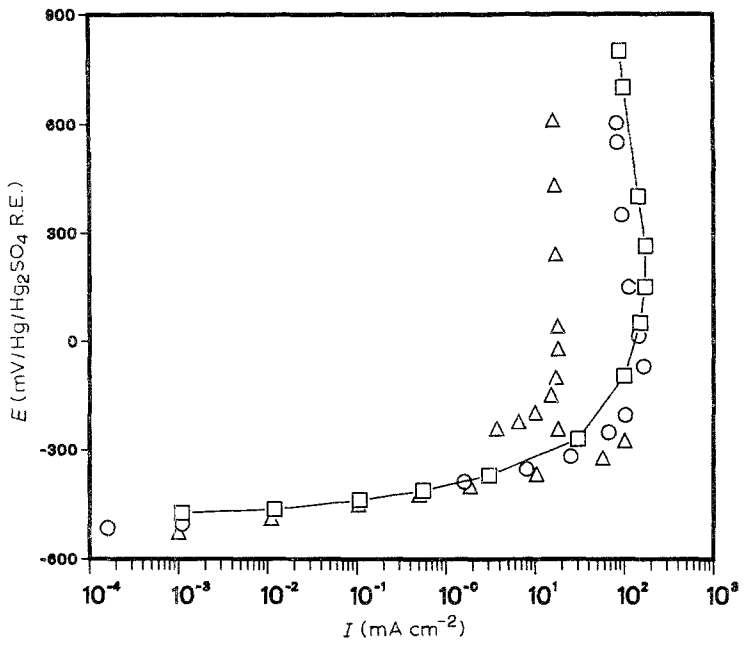

Fig. 5. Anodic polarization of pure copper in various acid concentrations. (□) 1.0, (○) 2.17 and (△) 9.44 N.

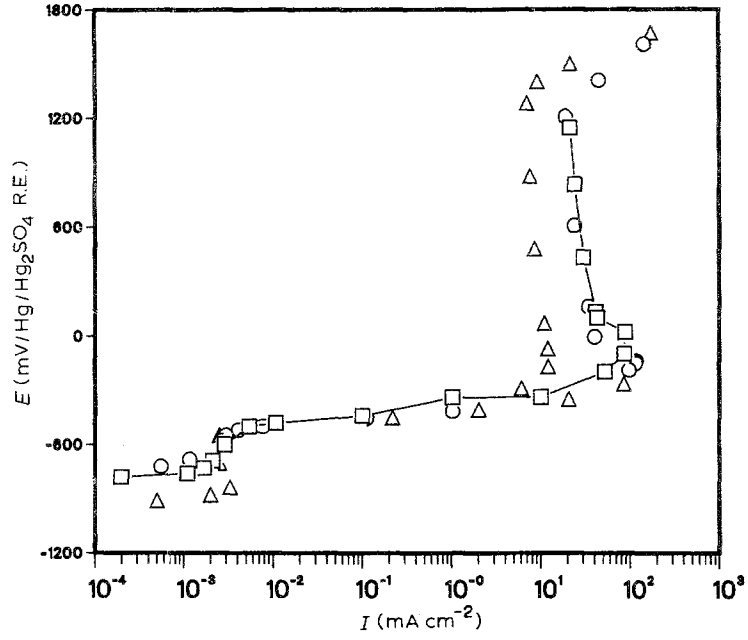

Fig. 6. Anodic polarization of Pb–63 wt % Cu in various acid concentrations. (□) 1.0, (○) 2.17 and (△) 9.44 N.

lead and lead alloys. I_c values for copper and Pb–Cu alloys decrease slightly with decreasing copper content. The I_c values are highest for 1.085 M acid for both pure copper and the monotectic alloy.

3. The I_p values are four orders of magnitude higher than those for lead or lead battery alloys. Hence, the process may be properly referred to as "pseudo-passivation". The I_p values (for Pb–63 wt % Cu) decrease with increasing acid concentrations, and they decrease with decreasing copper content.

4. Values of E_{pp} ("pseudo-passive" potential) are ~700 mV more positive than the normally observed passive potential for lead. For Pb–63 wt % Cu, E_{pp} decreases with increasing acid concentration.

5. For pure copper, the anodic Tafel slope is very low because of rapid copper dissolution. At all acid con-

Table 5. Quantitative results for anodic polarization of Pb and Pb battery-grid alloys in 4.72 M (9.44 N) acid

Parameter	*Units*	*Pure Pb*	*Pb–Ca*	*Pb–Ca–Sn*
Anodic Tafel Slope	mV decade^{-1}	12.83	11	12
I_c	mA cm^{-2}	0.671	0.306	0.722
E_{corr}	mV	−1050	−1050	−1046
E_{pp}	mV	−1008	−1020	−1006
I_p min	mA cm^{-2}	0.0022	0.0011	0.0016

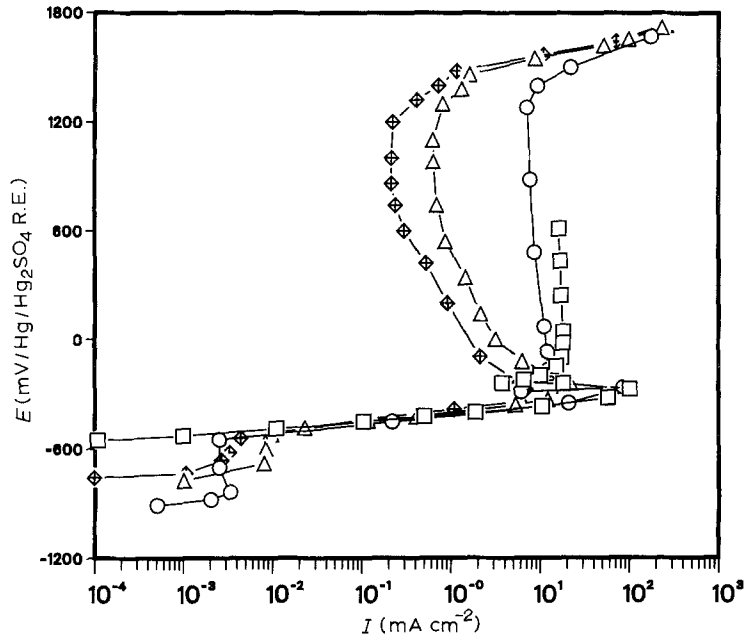

Fig. 7. Anodic polarization curves in 4.72 M (9.44 N) H_2SO_4 for as-polished (△) Pb–30 wt % Cu and (⊕) Pb–10 wt % Cu compared with (□) pure and monotectic (○) Pb–63 wt % Cu alloy.

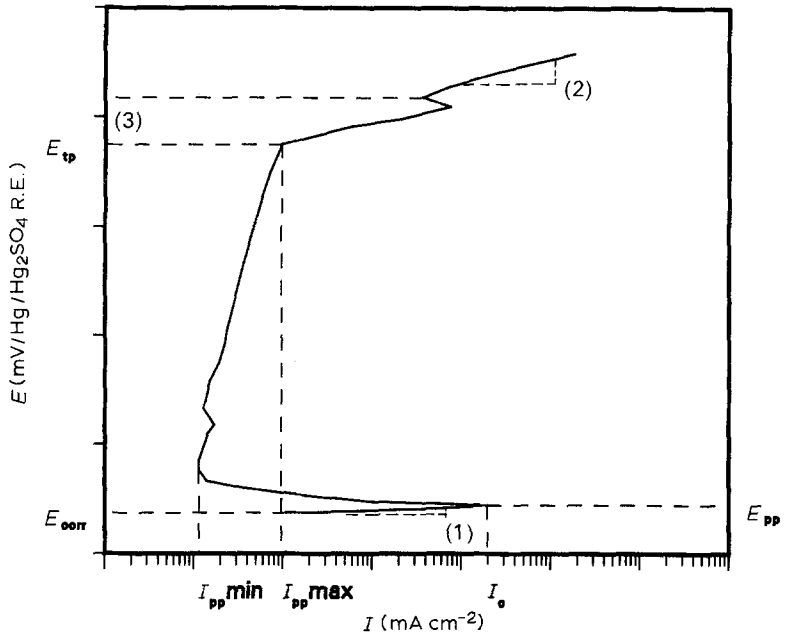

Fig. 8. Schematic anodic polarization curve showing parameters used for quantitative comparison of the data. Including (1) Anodic Tafel slope, (2) Slope of oxygen evolution curve, and (3) potential of oxygen evolution.

centrations, the Tafel slopes in the region of copper dissolution for the Pb–Cu alloys are slightly higher than that for pure copper. However, in all cases they are virtually independent of acid concentration.

3.3. *"Conditioned" Pb–30 wt % Cu alloy*

The surfaces of the leached Pb–30 wt % Cu after exposure for 60 000 s at 0 mV (now as Pb–30 wt % Cu "conditioned") showed $PbSO_4$ and copper crystals, and the rest-potential was close to that of pure copper, confirming the presence of copper on the surface even after leaching. The quantitative results are presented in Table 6, and Fig. 10 compares the behaviour of the as-polished and the "conditioned" nominal 30 wt % Cu alloy with that of pure copper and mono-

Table 6. Quantitative results for anodic polarization of Pb–30 wt % Cu and Pb–10 wt % Cu in comparison with pure Cu and Pb–63% Cu alloy in 4.72 M (9.44 N) acid

Parameter	*Units*	*Cu*	*Pb–63% Cu*	*Pb–30% Cu*	*Pb–10% Cu*	*Pb–30% Cu "Cond."*
Tafel slope in the region of copper dissolution	mV decade^{-1}	39	46	51.3	55.3	49.15
I_c	mA cm^{-2}	101	85.5	22.0	6.92	3.50
E^*_{corr}	mV	−572	−910	−774	−756	−478
E_{pp}	mV	−276	−266	−240	−274	−336
I_p min	mA cm^{-2}	17.4	9.20	0.62	0.21	0.41

* Values for Pb–Cu alloys are non steady-state. See Fig. 9.

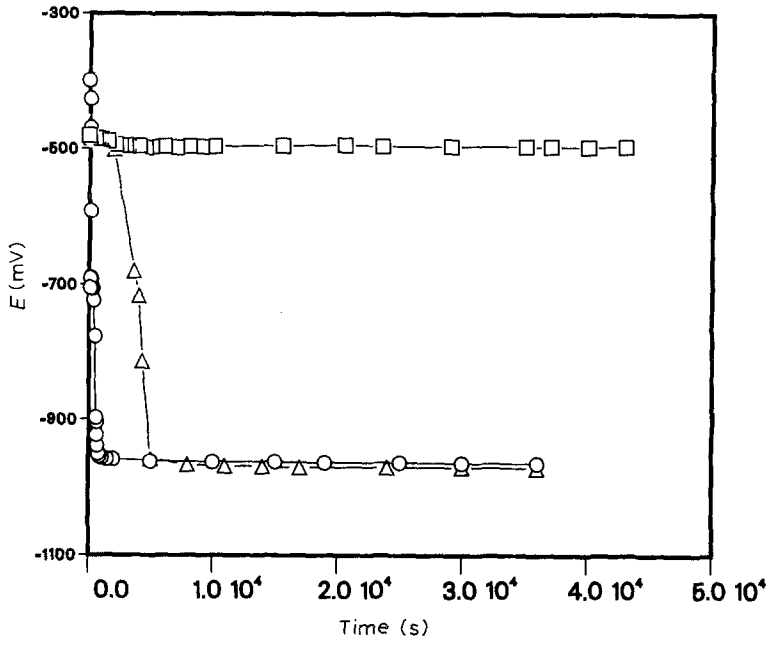

Fig. 9. Variation of open-circuit potential of Cu and Pb–Cu alloys with time in 0.5 M (1 N) H_2SO_4 [7]. (□) Pure Cu, (○) Pb–10% Cu, and (△) Pb–63% Cu.

tectic Pb–63 wt % Cu alloy. From SEM observations after anodic polarization, the surface of the conditioned 30 wt % Cu alloy appeared porous especially at the places where the aligned dendrites previously existed. To observe the corroded layer, the sample was transversely sectioned and polished. Figure 11a shows the transverse section of the aligned copper dendrites. Figure 11b, c, d show details of the corroded interface.

4. Discussion

4.1. *Electrodissolution of pure copper*

As shown in Figs 2–5 and Tables 3–6, the electrochemical behaviour of pure copper differs substantially from that of pure lead and lead battery alloys. The corrosion potential is in good agreement with estimates of the reversible potential for simultaneous satisfaction of the Cu/Cu^{2+} and Cu/Cu^{+} electrode reactions under conditions of saturation with $CuSO_4$, which also accounts for the decrease in corrosion potential with increasing acid concentration (i.e., an increase in acid concentration increases the sulphate ion activity with a corresponding decrease in Cu^{2+} and Cu^{+} concentrations.) In non-complexing solutions like sulphates, copper is found to occur predominantly in the divalent (Cu^{2+}) state [8]. The formation of passive films [consisting of CuO, Cu_2O or $Cu(OH)_2$] can be achieved in strongly acidic solution (e.g. 10 M H_2SO_4 acid) if the anodic reaction is driven sufficiently fast so that saturation of the dissolution product can be reached [8]. We believe that in our experiments, active dissolution of copper on anodic polarization leads to thickening of the $CuSO_4$ film. The decrease of the current at higher anodic potentials suggests a "pseudo-passivation" behaviour, with the rate of dissolution being controlled by ohmic effects and diffusion in the liquid.

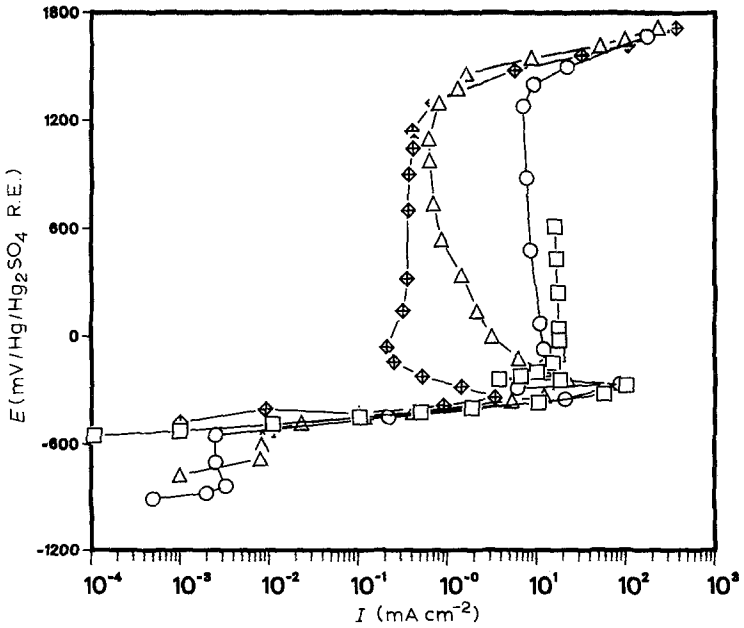

Fig. 10. Anodic polarization curves in 4.72 M (9.44 N) H_2SO_4 for (△, ⊕) Pb–30% Cu (as polished and "conditioned") compared with (□) pure Cu and (○) monotectic Pb–63 wt % Cu alloy.

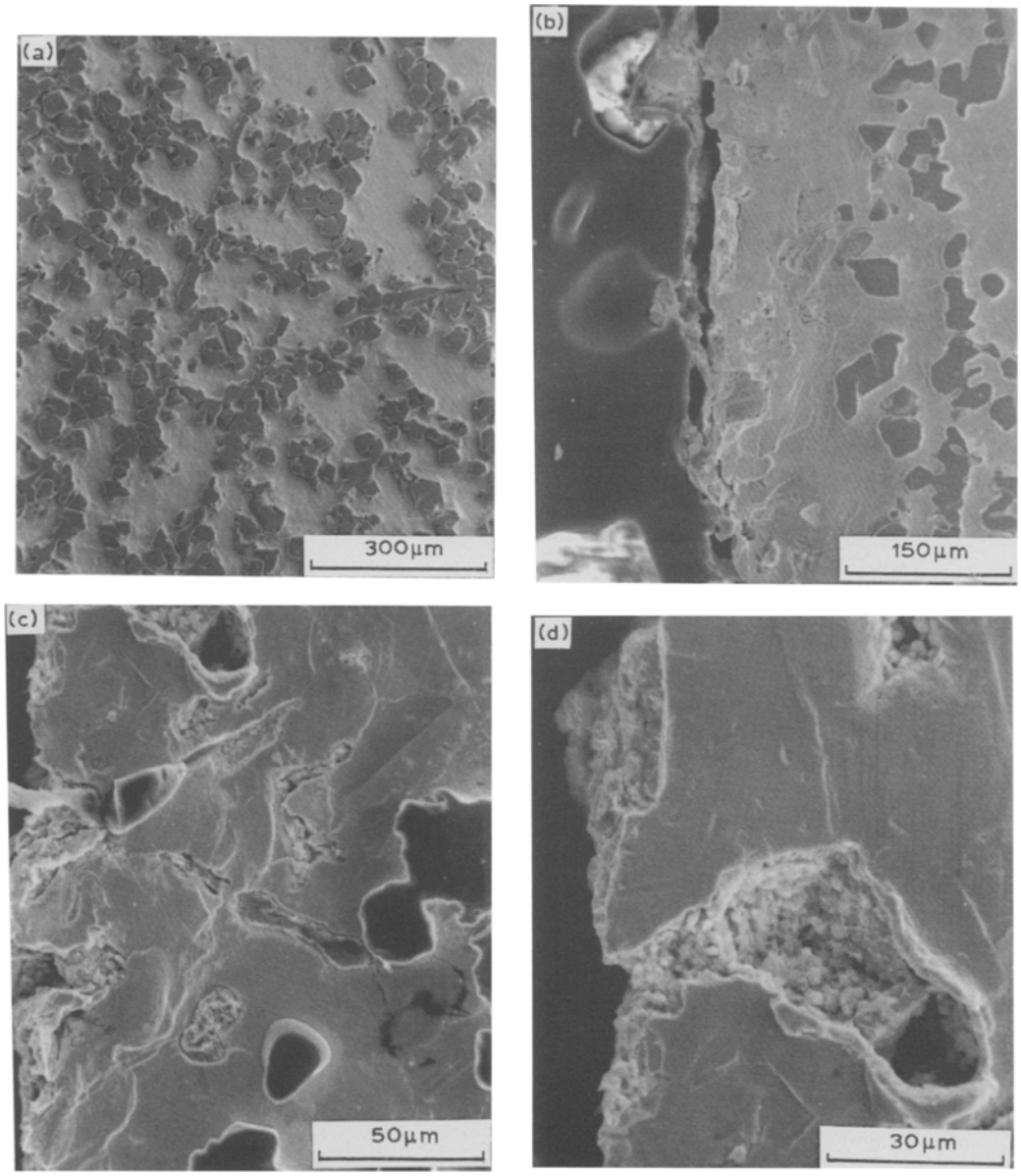

Fig. 11. Transverse section of "conditioned" Pb–30 wt % Cu anodically polarized in 4.72 M (9.44 N) H_2SO_4 following leaching at 0 mV for 60 000 s: (a) shows the copper dendrite distribution in the lead matrix; (b), (c), and (d), show the corroded interfaces at different locations and magnification.

4.2. *Corrosion behaviour of monotectic Pb–63 wt % Cu alloy*

The corrosion potential for all three Pb–Cu alloys is between that of pure lead and pure copper, and the subsequent polarization behaviour suggests that the alloys are initially passive, with a protective layer of $PbSO_4$ restricting lead dissolution in the presence of non-reacting copper. However, as discussed above, active behaviour of lead and establishment of the $Pb/PbSO_4$ potential occurs if sufficient time is allowed [7] as shown in Fig. 9. The anodic behaviour of the monotectic alloy is similar to pure lead until it reaches a critical potential where rapid copper dissolution occurs, giving rise to virtual selective removal of copper. The rapid dissolution of copper (virtually a non-polarizable reaction) leads to practical superposition of the polarization curves for the alloy and pure copper in this region. The same "pseudo-passive" transition is also observed with only a slight decrease in the passive current. Initial attempts to "condition" this alloy (for 60 000 s only and in the same electrolyte) to produce a copper-free porous lead surface layer were not successful. More recently however, we have succeeded in reducing the passive current by "conditioning" for a longer time (i.e. much greater than 60 000 s) and replenishing the cell with fresh electrolyte after every few thousand seconds, such that subsequent polarization approaches more closely to lead-like behaviour [7].

4.3. *Behaviour of hypermonotectic Pb–30 wt % Cu and Pb–10 wt % Cu*

These alloys show behaviour similar to that of the monotectic alloy. From Fig. 7 it can be concluded that the "pseudo-passive" current decreases with copper content in the alloy, although not proportionally, as

evident from quantitative values of I_p min in Table 6. The following inferences can be drawn from the large currents observed in the "pseudo-passive" region for Pb–30 wt % Cu and Pb–10 wt % Cu:

1. The surface copper content was sufficient to maintain a relatively high current during the anodic polarization.

2. All the surface copper could have dissolved at a relatively high potential leading to a highly porous surface. Due to the porous nature of lead after copper removal, a mechanically sound passive film may not have been able to form, leading to large currents mainly from the corrosion of lead.

3. After the copper dendrites exposed at the surface have been dissolved, lead films separating the latter from interior dendrites could be subsequently corroded away exposing a fresh copper surface which would then be subject to dissolution. This copper however, could be passivated by the formation of Cu_2O, CuO, or $Cu(OH)_2$ in the pores leading to relatively lower corrosion rates.

4.4. *Behaviour of "Conditioned" Pb–30 wt % Cu alloy*

After the conditioning treatment, and while the sample is removed from the electrolyte, it exists for a few seconds at the rest potential. There is a good possibility that the potential established could be sufficiently cathodic to promote Cu^{2+} reduction. Consequently, Cu can redeposit locally, which explains why fine copper grains were seen on the surfaces after leaching [6].

On subsequent polarization of the "conditioned" Pb–30% Cu (in a fresh 4.72 M solution) the rest potential assumes a value close to that of pure copper. (See Fig. 10.) This supports the presence of copper redeposited from the solution immediately after leaching.

As discussed previously, given sufficient time the potential would have dropped to a new value established by the lead sulphate/oxides formed during conditioning. The initial anodic current can be attributed to the dissolution of this redeposited copper. The relatively large passive currents could be a combined effect of some further copper dissolution and a surface area effect of lead matrix corrosion.

The transverse section of "conditioned" Pb–30 wt % Cu (Fig. 11a, b, c, and d) shows a uniform thickness of the corroded layer after anodic polarization. The dendrites in the interior are unaffected by the acid. The porous nature of the corroded interface (Fig. 11c and d) suggest that the large surface area may be responsible for the large passive currents. Analysis of the pores (EDS) shows that mainly lead was present in the space previously occupied by the copper dendrites. The little copper that was also found could have been redeposited. Hence, if during the leaching process, fresh solution were provided (the previous runs had a constant amount throughout the experiment), the surface copper could be removed completely without the

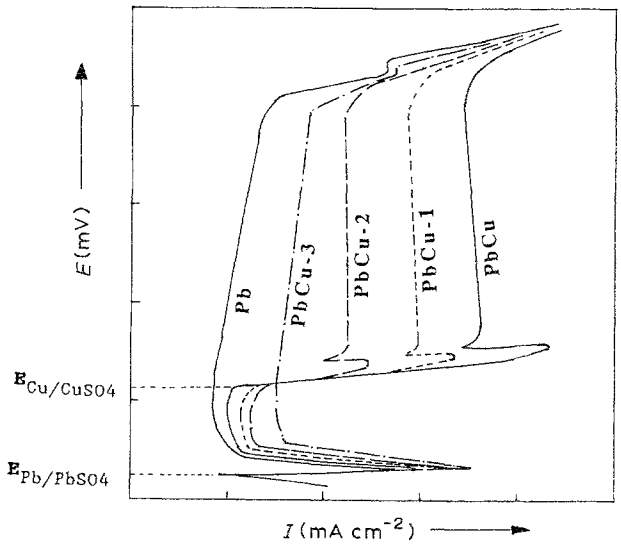

Fig. 12. Schematic polarization curves for Pb, Cu, and Pb–Cu alloy illustrating progressive effect of selective leaching of copper.

fear of redeposition, and lead-like behaviour would attain on subsequent polarization. Such an effect is shown schematically in Fig. 12: Given sufficient time to establish the $Pb/PbSO_4$ rest potential, the Pb–Cu alloy shows initially a lead-like behaviour, but once the Cu/Cu^{2+} reversible potential is reached, it shows the behaviour of pure copper. Progressive selective leaching affects the subsequent polarization behaviour by reducing the current due to copper dissolution above the Cu/Cu^{2+} reversible potential. (See Fig. 12, curves Pb–Cu 1, 2, 3.) Thus, the remaining current is not governed by copper dissolution but arises from oxidation of lead under conditions of greatly increased surface area. Such a behaviour has been observed for Pb–10% Cu alloy [7]. More work is in progress.

5. Conclusions

1. Copper does not undergo normal passivation in acid–sulphate media but corrodes rapidly on anodic polarization, displaying a "pseudo-passive" transition at high anodic potentials. The open-circuit (corrosion) potential is close to the Cu/Cu^{2+} reversible potential in this media.

2. Monotectic Pb–63 wt % Cu is metastable-passive at an open circuit potential which lies between that of pure copper and lead. This potential is a non-steady state value which eventually decays to the reversible potential of lead. Above the open-circuit potential for pure copper, the anodic behaviour of the monotectic alloy is similar to that of pure copper, including the appearance of the "pseudo-passive" transition. Selective dissolution of copper from the alloy occurs, leaving a porous network of lead on the surface.

3. Similar behaviour occurs in the alloys with lower copper content (30 wt % and 10 wt % Cu), which, however, display smaller anodic currents in the pseudo-passive region. Long-time potentiostatic selective leaching of copper from the 30 wt % Cu alloy produced a highly porous layer of spongy lead and lead

sulphate; the subsequent anodic polarization behaviour (without repolishing the sample surface) showed that the pseudo-passive current decreases from ~ 0.4 to $\sim 0.2\,mA\,cm^{-2}$ or ~ 20 times greater (referred to unit geometric area) than the passive current of pure Pb and lead battery-grid alloys. This difference was attributed partly to dissolution of redeposited copper but mainly to the large effective surface area of the remaining porous lead network.

4. The possibility of using composite Pb–Cu alloys to achieve a useable battery grid with improved conductivity depends on improving the selective leaching process, including replenishing the cell with fresh electrolyte to prevent redeposition of copper.

Acknowledgements

The authors wish to acknowledge helpful discussions with Professor W. F. Flanagan as well as technical assistance by Mr G. Walker, all of Vanderbilt University. We also wish to thank Mr V. Dantam and (the late) Mr J. Barrick of General Motors/Delco Remy for their invaluable help. This work was sponsored by the NASA Office of Commercial Programs.

References

[1] J. D. Livingston, *Mater. Sci. Eng.* **7** (1971) 61.
[2] J. D. Livingston and H. E. Cline, *Trans. TMS-AIME* **245** (1969) 351.
[3] J. W. Cahn, *Met. Trans. A* **10A** (1979) 119.
[4] R. N. Grugel and A. Hellawell, *ibid.* **12A** (1981) 699.
[5] S. Shah, R. N. Grugel and B. D. Lichter, *Metall. Trans. A* **19A** (1988) 2677.
[6] S. Shah, B. D. Lichter, V. Dantam, *B. Electrochem.* **3**, No. 6 (1987) 565; S. Shah, M. S. Thesis, Vanderbilt University (1988).
[7] A. Rawat, M. S. Thesis, Vanderbilt University, Nashville, TN (1990).
[8] U. Bertocci and D. R. Turner, "Copper", 'Encyclopedia of Electrochemistry', Vol. II, Marcel Dekker, New York (1973) 383.